Ensemble forecast experiments of thunderstorm that occurred in the Kanto Plain on 13th Oct. 2010

Hiromu Seko, Osamu Suzuki, Kazuo Saito (Meteorological Research Institute),
Takemasa Miyoshi (University of Maryland)

1. Introduction

In the last decade, local heavy rainfalls generated in urban areas, such as the Tokyo Metropolitan area, have caused urban flush floods and influenced urban functions (e.g. Zoushigaya local heavy rainfall in 2008). To mitigate the damages from local heavy rainfalls, mechanisms of their developments and movements are needed to be understood. Because local heavy rainfalls are generally generated in mesoscale convergence zones, mesoscale convergences should be reproduced, as well as convection cells. To express mesoscale convergences and convection cells simultaneously, the two-way nested Local Ensemble Transform Kalman Filter (LETKF) system has been developed. In this report, an outline of the nested LETKF system and the assimilation results of the thunderstorm that was developed in the Kanto Plain on 13th October 2010 are explained.

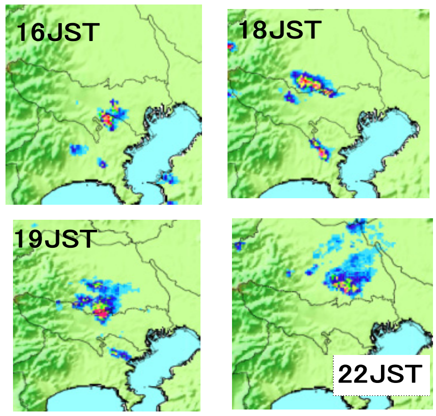

Fig. 1: Rainfall distributions of 13th October 2010 observed by conventional radars of JMA.

2. Thunderstorm developed on 13th Oct. 2010 in the Kanto Plain

Figure 1 shows the rainfall distributions from 16 JST (Japan Standard Time, 9 JST corresponds 0 UTC) by the operational radar of the Japan Meteorological Agency (JMA). New convections that were generated at the southern part of Tokyo by 16 JST moved northward and generated new cells on this northern side. These rainfall regions stayed at the northern part of Tokyo for more than 2 hours. After 21 JST, these rainfall regions moved northeastward and decayed while extending weak rainfall regions northeastward. Figure 2 shows the equivalent potential temperature and sea surface temperature at 20 JST and 23 JST. At 20 JST, the thunderstorm developed at the northern edge of the high equivalent potential temperature airflow from the south. Because the temperature was not much higher than that of the area around the developing point of the thunderstorm, it is deduced that the humid airflow from the south developed it. At 23 JST, a northerly wind region expanded to the south of the rainfall region. Because the moist airflow from the south could not be supplied into the thunderstorm directly, the thunderstorm began to decay. These distributions indicate low-level humid airflow is important for the development and decay of thunderstorms.

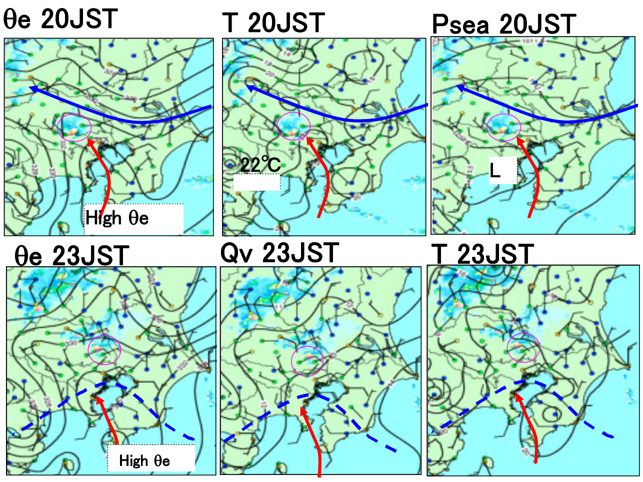

Fig. 2: Surface distributions of equivalent potential temperature, surface temperature, water vapor and sea level pressure at 20 JST and 23 JST13th October 2010.

3. Outline of experiments using the Nested LETKF system

Figure 3 is a schematic illustration of the nested LETLF system. To reproduce mesoscale convergences and convection cells, the nested system was composed of two NHM-LETKFs (Miyoshi and Aranami, 2006): Outer and Inner LETKFs. The horizontal grid intervals of the Outer and Inner LETKFs were 15 km and 1.875 km, respectively. In the Outer LETKF, the conventional data that was used in the JMA data assimilation system was

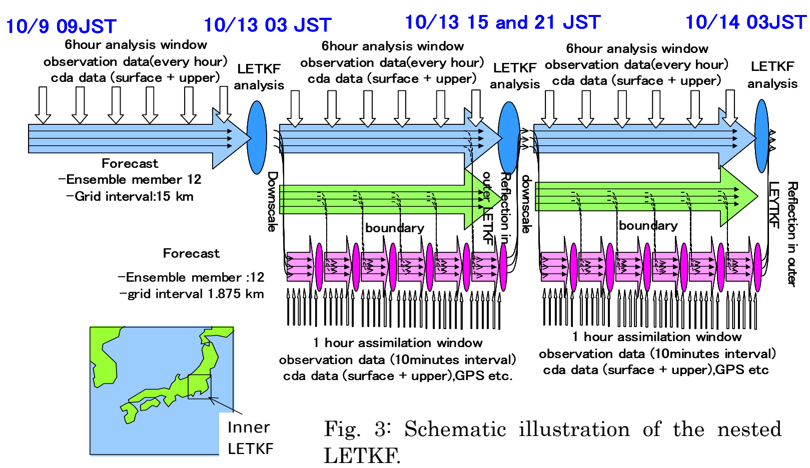

Fig. 3: Schematic illustration of the nested LETKF.

assimilated every hour. The conventional data and GPS-derived PWV data were assimilated every 10 minutes in the Inner LETKF. Assimilations of the Outer and Inner LETKFs were performed from 09 JST 9th October and 03 JST 13th October, respectively.

4. Results of ensemble analyses by the nested LETKF system

Figure 4 shows the ensemble mean and spread of the 1-hour rainfall amount and surface horizontal wind reproduced by the Inner LETKF. Southerly flow from the south converged with easterly flow that covered the northern part of Kanto Plain at 18 JST, and then convection cells **A** were developed at .the convergence area. This convergence area moved northward and other intense convection cells **B** were developed at the northwestern edge of southerly flow. At 24 JST the northerly wind region expanded south of the rainfall region and then the convection cells decayed. This simulated evolution is similar to the observed one, though the position of the reproduced convection cells **B** was shifted northward. However the spread around the convection **B** was too small to correct the position of convection cells **B**. It is deduced that the spread had already become smaller in the Outer LETKF. Other high-resolution data, such as radial wind of Doppler radar is needed to correct the position of convection cells **B**.

In addition to the conventional data, GPS-derived PWV data was assimilated in the Inner LETKF. When PWV data was assimilated, convection cells **A** became more intense and the convection cells **C** were generated near the eastern part of the Kanto Plain (Fig. 5). Because the convection cells **C** was not observed by radars (Fig. 4), PWV data is not sufficient and some other data, such as Doppler radar data, is needed to improve the rainfall forecast of this event.

At 22 JST, a significant vortex was generated near convection cells **B**. Figure 6 shows the mixing ratio of rain and horizontal wind at z=400 m. In three members, significant vortices were generated near the rainfall regions. Although the intensities of the vortices were weak, the vortex near the southwestern tip of the rainfall region was observed by Doppler radar (Fig. 7). The relationship of the rainfall region and vertex reproduced by ensemble member #000 was similar to the observed one. This result indicates the nested LETKF system has the potential to reproduce vortices that may cause tornadoes.

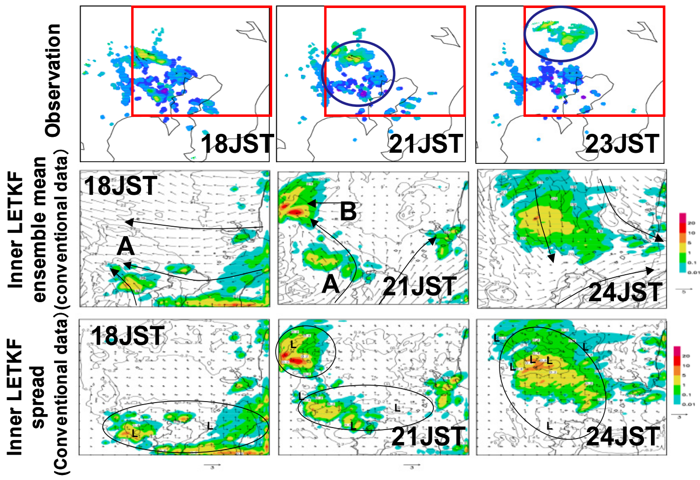

Fig. 4: (upper) Radar echo from 18 JST to 23 JST. (middle) and (lower) Ensemble mean and spread of 1 hour rainfall amount and surface horizontal wind reproduced by Inner LETKF.

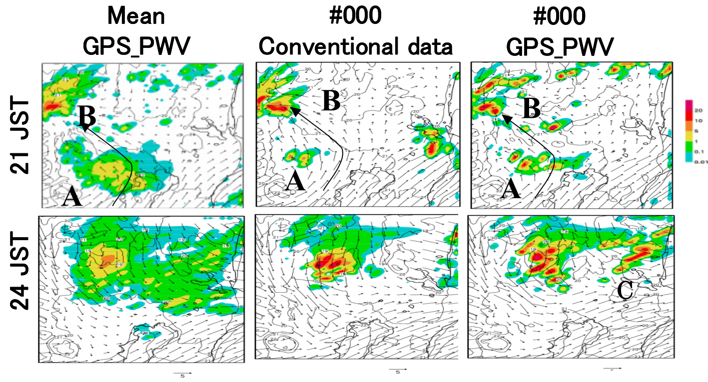

Fig. 5: Ensemble mean and analyses of #000 of 1 hour rainfall amount and surface horizontal wind reproduced by assimilation of convectional data and GPS-PWV data.

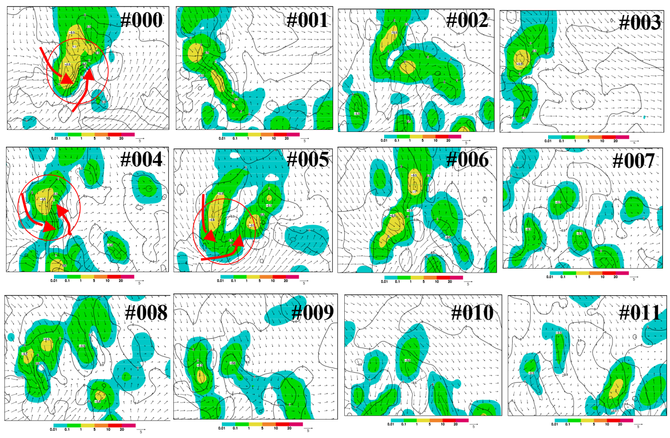

Fig. 6: Mixing ratio of rain at z=20 m and horizontal wind at z=400 m reproduced by assimilation of conventional data.

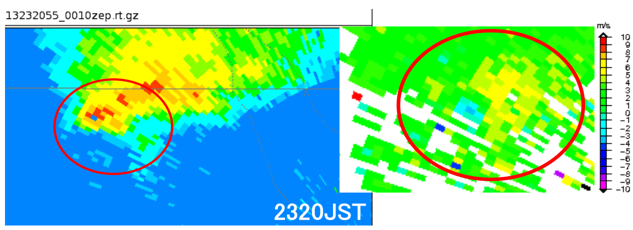

Fig. 7: Radar echo and radial wind at 2320 JST observed by the Tokyo radar..

Acknowledgements

The authors would like to express their gratitude to the Geospatial Information Authority of Japan and Observations Department of JMA, which provided the QZS position data, GPS data and Doppler radar data. The improvements of severe weather forecasts (i.e. local heavy rainfalls), which were achieved by the assimilations of Doppler radars, will contribute to aviation safety and the mitigation of damages of other urban functions.

Reference

Miyoshi, T. and K. Aranami, 2006: Applying a four-dimensional local ensemble transform Kalman filter (4D-LETKF) to the JMA nonhydrostatic model (NHM). SOLA, 2, 128-131.